Low-frequency dynamic wake meandering: comparison of FAST.Farm and DIWA software tools

Low-frequency dynamic wake meandering: comparison of FAST.Farm and DIWA software tools

I Rivera-Arreba[1], L Eliassen[2], E E Bachynski[1] and B Panjwani[3]

[1]Department of Marine Technology, Norwegian University of Science and Technology, Trondheim, Norway
[2] Department of Ships and Ocean Structures, SINTEF Ocean, Trondheim, Norway
[3] Department of Metal Production and Processing, SINTEF Industry, Trondheim, Norway

E-mail: irene.rivera.arreba@ntnu.no

Abstract. Most of the global dynamic response models used today for the design of wind turbines are based on the aero-hydro-servo-elastic analysis of one single turbine. However, research on bottom-fixed offshore wind turbines has shown that interactions among turbines in a farm influence both the power production and the structural loading. Furthermore, floating wind turbines (FWTs) are sensitive to low-frequency variations, and therefore to wake meandering perturbations. In the current work, we use the Dynamic Wake Meandering (DWM) model as implemented in DIWA and FAST.Farm, to study the low-frequency content of the meandering at a target turbine placed 8 diameters downstream. At frequencies in the range of the natural frequencies of rigid body motions of semisubmersible floaters, the two models yield different results. These differences are seen for every wind speed and wind turbine model, even though they decrease as the wind speed increases. The observed differences may affect low-frequency motions and consequently mooring system design.

1. Introduction

To achieve a fully economically viable way to harness wind energy in intermediate and deep water depths, further cost reductions and design improvements are needed in the floating wind energy industry. With two operating floating wind farms, Hywind Scotland and WindFloat Atlantic, and others under development, it is increasingly important to understand wake interactions in a farm [1].

Downstream wind turbines experience both a decrease in the mean wind speed and an increase in turbulence intensity compared to upstream turbines. To account for the effect of wakes in wind farms, several steady or quasi-steady models have been applied so far, both onshore and offshore. However, the wake downstream of a turbine is unsteady and it meanders. This wake meandering is related to the random unsteady transverse oscillations of the mean velocity deficit around the time-averaged centreline. These oscillations are caused by very large turbulent eddies, larger than the turbine rotor, in the incoming atmospheric boundary layer (ABL), as firstly observed by Ainslie [2] and later confirmed experimentally by España et al. [3].

Until recently, if one wanted to account for dynamic effects, computationally demanding large-eddy simulations (LES) had to be performed. The Dynamic Wake Meandering (DWM) model was proposed by Larsen et al. [4] and describes the wake as a passive tracer driven by the large-scale turbulence structures in the ABL. This medium-fidelity engineering model accounts for the wake expansion and its dynamic movement with sufficient accuracy at a low computational cost. The DWM model coupled to HAWC2 [5], an aeroelastic code to compute the response of wind turbines

in time domain developed at DTU, has been validated against operational wind farm measurement data [6, 7].

Since 2019, the DWM is included in the revised IEC standard [8] as a recommended practice to account for wake effects from neighbouring turbines in a wind farm. Based on the fundamental idea of turbulence scale splitting, Larsen et al. [4] proposed a *cut-off eddy size*, so that turbulent eddies smaller than two rotor diameters affect the wake deficit evolution and those larger than two rotor diameters affect the wake meandering. Accordingly, the model consists of three submodels:

(i) **Wake** (or velocity) **deficit**, described in the meandering frame of reference,

(ii) a stochastic model of the downstream **wake meandering** process and

(iii) the **added-wake turbulence** (or self-induced wake turbulence), described in the meandering frame of reference.

In the DWM model, the wake-deficit is based on the thin shear-layer approximation of the Reynolds-averaged Navier-Stokes equations under quasi-steady-state conditions in axisymmetric coordinates, with the turbulence closure captured by using an eddy-viscosity formulation. The thin shear-layer approximation neglects the pressure term and assumes that the velocity gradients are much bigger in the radial direction than in the axial direction. The velocity deficit in the far-wake region is modelled by Equation 1:

$$U\frac{\partial U}{\partial x} + V_r\frac{\partial U}{\partial r} = \frac{\nu_T}{r}\frac{\partial}{\partial r}\left(r\frac{\partial U}{\partial r}\right), \tag{1}$$

where U is the axial velocity component, V_r the radial velocity component, r the radial coordinates and ν_T the eddy viscosity. The eddy viscosity is modelled by the filter parameters F_1 and F_2, described and calibrated by Madsen et al. [9], and extended by Larsen et al. [4] and Keck [10].

More recently, the DWM model was implemented in FAST.Farm [11], an extension of the aero-hydro-servo-elastic tool OpenFAST developed by the National Renewable Energy Laboratory (NREL). Similarly, SINTEF Ocean and SINTEF Industry developed DIWA (Disturbed Inflow Wind Analyzer) [12], which can be used within the workbench SIMA, the numerical tool to model the response of marine structures developed at SINTEF Ocean. The DWM model in DIWA follows a very similar approach to that of HAWC2, based on Madsen's model [9].

In the current work, we use FAST.Farm and DIWA to study the effects of an upstream wind turbine on a target turbine placed 8 diameters (D) downstream. We focus on the low-frequency component of the wake meandering path due to its relevance for floating wind turbine motions. Both FAST.Farm and DIWA are used to study three fixed wind turbine models increasing in rotor size: the NREL5MW [13], the DTU10MW [14] and the INO WINDMOOR 12MW (WM12MW) [15]. The incoming wind field is generated using the Mann turbulence model, and three representative mean wind speed conditions (below-rated, rated and over-rated) are applied.

A description of the DWM models, the turbine models used throughout this work and the main parameters used to generate the synthetic turbulent inflow are described in Section 2. The effect of using FAST.Farm or DIWA to compute the deficit and the meandering is presented in Section 3. Furthermore, the effects of shaft tilt, precone, and a shear profile in FAST.Farm are briefly discussed. Section 4 presents the conclusions and further work.

2. Methodology

2.1. DWM models

FAST.Farm is a multiphysics engineering tool composed of several submodels, which account for different physical processes within a wind farm. FAST.Farm uses NREL's OpenFAST to solve the aero-hydro-servo-elastic dynamics of each turbine, but considers additional physics for the wind field across the wind farm in the ABL. The aerodynamic loads on the blades are computed using blade

element momentum theory. Even though FAST.Farm is based on the principles of the DWM model, it addresses many of the limitations of previous DWM implementations, as explained in FAST.Farm's theory manual [11]. FAST.Farm does not include added-wake turbulence, but its contribution to the total turbulence is smaller and therefore the effect on wake meandering in the region of interest, the far-wake, is low: ambient turbulence tends to dominate in the far-wake region [9, 16].

LES was used to validate FAST.Farm [17], and to calibrate certain wake dynamics parameters [18], accounting for stable, neutral and unstable atmospheric conditions. Shaler et al. [19] studied the effects of varying spatial and temporal discretization of the wind domains on the low- and high-resolution domain, which are used as input in FAST.Farm. The current work follows the recommendations on the spatial and temporal discretization from Shaler et al. [19].

DIWA consists of three major submodels, which correspond to the three DWM submodules described in Section 1. Consistently, three turbulence boxes are needed as input: the ambient, the added-wake turbulence and the meandering wind field boxes. A brief description of DIWA implementation can be found in the work of Panjwani et al. [20], where the model was benchmarked against literature data.

Table 1 gives an overview of the main differences between the two programs. One difference that is not retrieved in Table 1 is the modelling of the eddy-viscosity (see Equation 1), which is also expected to affect the responses of the wind turbines [20]. DIWA has four deficit models implemented, with most of the parameters already hard-coded. The four models are based on the work of Madsen [9], Larsen [4], Keck [10] and the most recent one, developed and included in the IEC standards [8]. The third and fourth models allow for implementing the Monin-Okhunov length scale parameter, related to atmospheric stability [21]. In the current work this length scale corresponds to neutral atmospheric stability. FAST.Farm allows the user to calibrate the parameters which affect the eddy-viscosity formulation. In this work, the parameters are set based on the calibration against LES by Doubrawa et al. [18].

Table 1: DIWA and FAST.Farm main differences.

	FAST.Farm	**DIWA**
Wake propagation	The wake follows the disturbed flow. The fluctuating longitudinal wind speed is included.	The wake is moved with the mean wind speed. The fluctuating longitudinal wind speed is not included.
Shear profile	Contains a shear profile.	There is no shear included.
Wind files	Uses one wind file for estimating both velocity deficit and for the meandering path. No added-wake.	Needs three input files: meandering, deficit and added turbulence.
Wind turbine	Coupled with OpenFAST. Can include elasticity, yaw and tilt angles, and platform motions.	Stand-alone program. Uses stiff blades, no yaw angle and no tilt of the rotor.

2.2. Wind turbine models

Three wind turbine models with increasing rotor diameter have been used: the NREL5MW, the DTU10MW and the INO-WINDMOOR 12MW. Table 2 presents the main characteristics of the three models. In the present work, to better compare the two frameworks, the support structure is fixed, and the blades and the tower are rigid, with no shaft tilt or precone.

2.3. Inflow wind field generation

In the present work, we use the Mann spectral tensor model for generating turbulent wind fields. The main parameters for generating the wind field boxes for the three cases are shown in Table 3. The

Table 2: Main characteristics of the three wind turbine models.

	NREL5MW	**DTU10MW**	**WM12MW**
Rotor diameter [m]	126	178.3	216.9
Hub height [m]	90	119	131.7
Rated power [MW]	5	10	12
cut-in, rated, cut-out wind speed [m/s]	4, 11.4, 25	4, 11.4, 25	4, 10.9, 25
cut-in, rated rotor speed [rpm]	6.9, 12.1	6.0, 8.7	5.5, 7.8

necessary input data, namely the non-dimensional shear distortion parameter γ, the length scale parameter L and the turbulent kinetic energy parameter $\alpha\epsilon$ are calculated based on the IEC61400-1 recommendations [8]. The turbulence intensity (TI) is chosen to be 5.6 % based on the measurements from the FINO1 platform [22]. Furthermore, the wind profile is constant, i.e. no shear is applied in any of the programs, since the available version of DIWA does not allow for a sheared wind profile. In total, six seeds have been used for each wind field for every mean wind speed (U). Each realisation is 4096 s long, and we analyse one-hour simulations, after a 496 s transient time span.

Table 3: Simulation parameters.

Parameter	γ [-]	L [m]	$\alpha\epsilon^{2/3}$ [m$^{4/3}$/s^2]	σ_{iso} [m/s]	σ_1 [m/s]
Value	3.9	33.6	$55 \cdot \frac{0.4754}{18} \cdot \sigma_{iso}^2 \cdot L^{-2/3}$	$\frac{\sigma_1}{\sqrt{3.25}}$	U$\cdot$ TI

To compare both frameworks, we have used the same ambient wind field input files, for each wind speed and model, respectively. The low-resolution (low-res) domains are different for the two frameworks. Figure 1 illustrates the high- and low-res domains in FAST.Farm and the ambient and meandering wind boxes in DIWA, viewed from above, with the mean wind speed in the positive x direction. For clarification, the high-res domain in FAST.Farm coincides with the ambient wind field in DIWA, whereas the low-res domain in FAST.Farm is analogous to the meandering wind field box in DIWA. The high-res domain, in blue in Figure 1 is the same for both FAST.Farm and for DIWA, and has the same resolution dSHigh (dyHigh and dzHigh). However, in DIWA the low-res parameter dSLow (dyLow and dzLow) corresponds to the spatial resolution of the meandering wind box (right, top, red-dotted figure in Figure 1), whereas in FAST.Farm it is the resolution of the low-res domain, which is down sampled from the high-resolution (or ambient wind field) domain.

The characteristics of the ambient wind field box are shown in Table 4. The spatial resolution in y and z, dS, has been chosen based on the chord length of the respective turbine models: 5 m for the NREL5MW and 7.5 m for the DTU10MW and the WM12MW. The resolution in the x-direction, dx, has been chosen based on the mean wind speed, and on the recommended time step for both frameworks. The number of grid points in the three directions nx, ny and nz have been determined based on the required dimensions to capture meandering properly.

Table 5 in Appendix 4, gives an overview of the wind field resolution parameters used throughout this work, normalised by the rotor diameter, and compared to the recommended values, for FAST.Farm [19] and DIWA [12]. The high- and low-res parameters are indicated with *High* and *Low*.

3. Results

3.1. Deficit

Figure 2 presents the wake deficit for the three wind turbine models at the target turbine placed 8D downstream of the first wind turbine.

The first observation from Figure 2 is the significant difference among the four models implemented in DIWA, more specifically between *DIWA; Keck* and *DIWA; Madsen* and FAST.Farm,

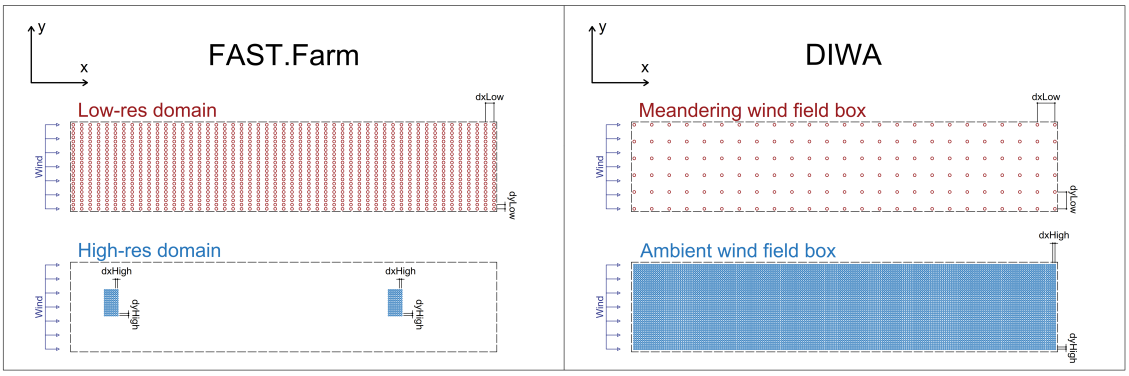

Figure 1: Left: FAST.Farm sketch of the high (or ambient wind field)- and low (or meandering wind field)- resolution domains. Right: DIWA sketch of the ambient (high-res) and meandering (low-res) wind field boxes.

Table 4: Parameters of the ambient (high-res) turbulence box for both programs and for the three wind turbine models.

Parameter	**8m/s**	**11.4m/s**	**15m/s**
dx [m]	2.00	2.85	3.75
dS - NREL5MW [m]	5.0	5.0	5.0
dS - DTU10MW and WM12MW [m]	7.5	7.5	7.5
nx [-]	16384	16384	16384
ny [-]	256	256	256
nz [-]	128	128	128

at a mean wind speed (WS) of 8 m/s. The high deficit resulting from Madsen's implementation was reported previously, especially when having moderate to high spacing between turbines and combined with low TI [6]. The difference between the models decreases as the wind speed increases. Secondly, even though the effect is not as remarkable, for the largest turbine model, the WM12MW, the wind speed recovery is greater than the for the smallest, the NREL5MW.

3.2. Meandering

Figure 3 shows the main statistical parameters of the horizontal (subfigures on top) and vertical (subfigures at the bottom) meandering patterns at the target turbines: the NREL5MW (red), the DTU10MW (green) and the WM12MW (blue). The statistical parameters are based on 1-hour time length simulations. The statistical values are normalised by the rotor diameter. Furthermore, for the vertical meandering, the hub height is subtracted, so that a mean value of zero coincides with the hub height. The open symbols show each of the realisations, and the dashed and point-dashed lines represent the average value of the six realisations for each case, for FAST.Farm (FF) and DIWA, respectively.

For both horizontal and vertical meandering, the standard deviation stays relatively constant with respect to the wind speed. In general, FAST.Farm shows a higher standard deviation than DIWA. The difference is larger for the horizontal meandering, which is consistent with the observed maximum and minimum values of the meandering. Note that there is no tilt of the shaft, or precone angle, or pitch of the substructure, so the wake does not deflect upward.

Figures 4 and 5 show the power spectral density (PSD) of the horizontal and vertical normalised wake center position, respectively, for the two programs, at the target turbine placed 8D downstream.

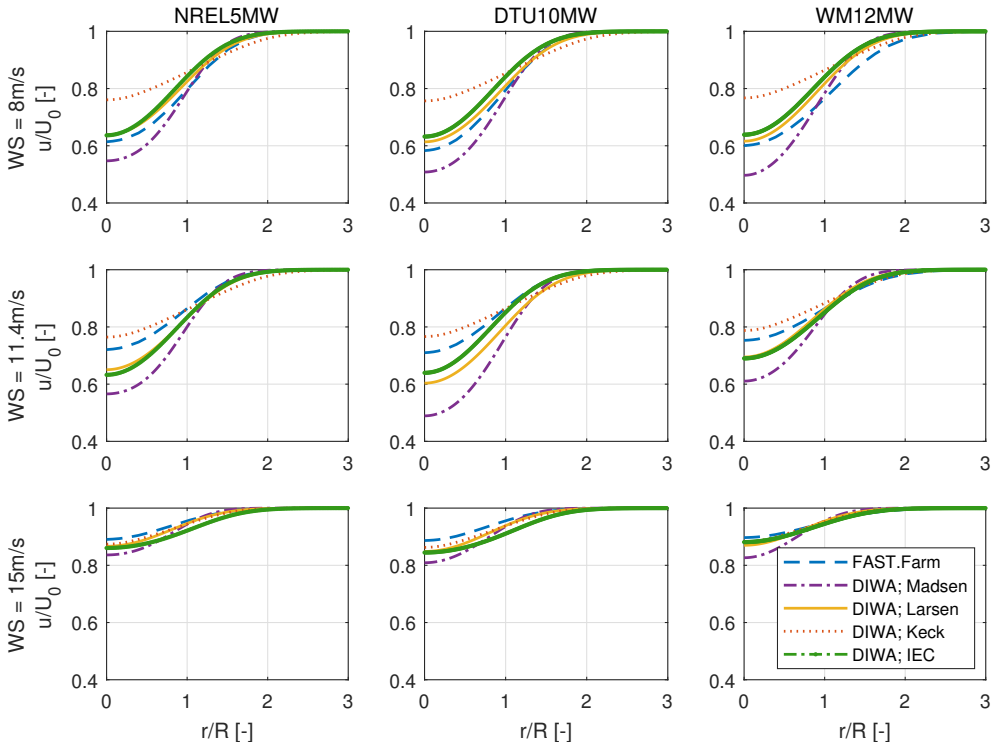

Figure 2: Wake deficit at the target turbine placed 8D downstream the first wind turbine. Left: NREL5MW, middle: DTU10MW, right: WM12MW. Top: 8 m/s, middle: 11.4 m/s, bottom: 15 m/s.

From top to bottom, the rows of subfigures correspond to the 8 m/s, 11.4 m/s, and 15 m/s cases. The columns correspond to the NREL5MW model, the DTU10MW model, and the WM12MW model. The lighter lines correspond to the six realisations for each program, and the dark lines correspond to the average of these seeds: in blue for FAST.Farm, and in red for DIWA. To relate the low-frequency content with the usual natural frequencies of floating wind turbines, the vertical lines represent the surge (f_1), pitch (f_5), yaw (f_6) and heave (f_3) natural frequencies of three representative semisubmersible floaters for the respective rotor sizes: the OC5-semisubmersible [23], the Life50+ Nautilus semisubmersible [24] and the INO-WINDMOOR semisubmersible [15]. The eddy-viscosity model used with DIWA for the figures shown here is the one implemented by Keck. However, as expected from the DWM formulation, the steady-state deficit model does not affect the meandering pattern.

In general, there is lower meandering in DIWA than in FAST.Farm, consistently with the standard deviation in Figure 3. The largest difference is seen for the smallest rotor size, the NREL5MW, for the horizontal meandering, and the WM12MW for the vertical meandering. As the wind speed increases, this difference is decreased. Furthermore, as the wind speed increases, the meandering decreases for both models.

A possible explanation for the differences in the energy content between FAST.Farm and DIWA is the treatment of the wind input. While the low-res domain in FAST.Farm is down sampled from the ambient wind field, DIWA uses a separately generated meandering (lower resolution) wind field box, which is also statistically independent from the ambient wind field. Furthermore, the recommended resolution of the two wind files used to account for meandering differs, as shown in Table 5. Another major difference is that FAST.Farm uses the disturbed turbulence field, i.e. ambient and meandering field, to estimate the meandering behavior.

In an attempt to justify this hypothesis, we ran DIWA with the meandering wind field down

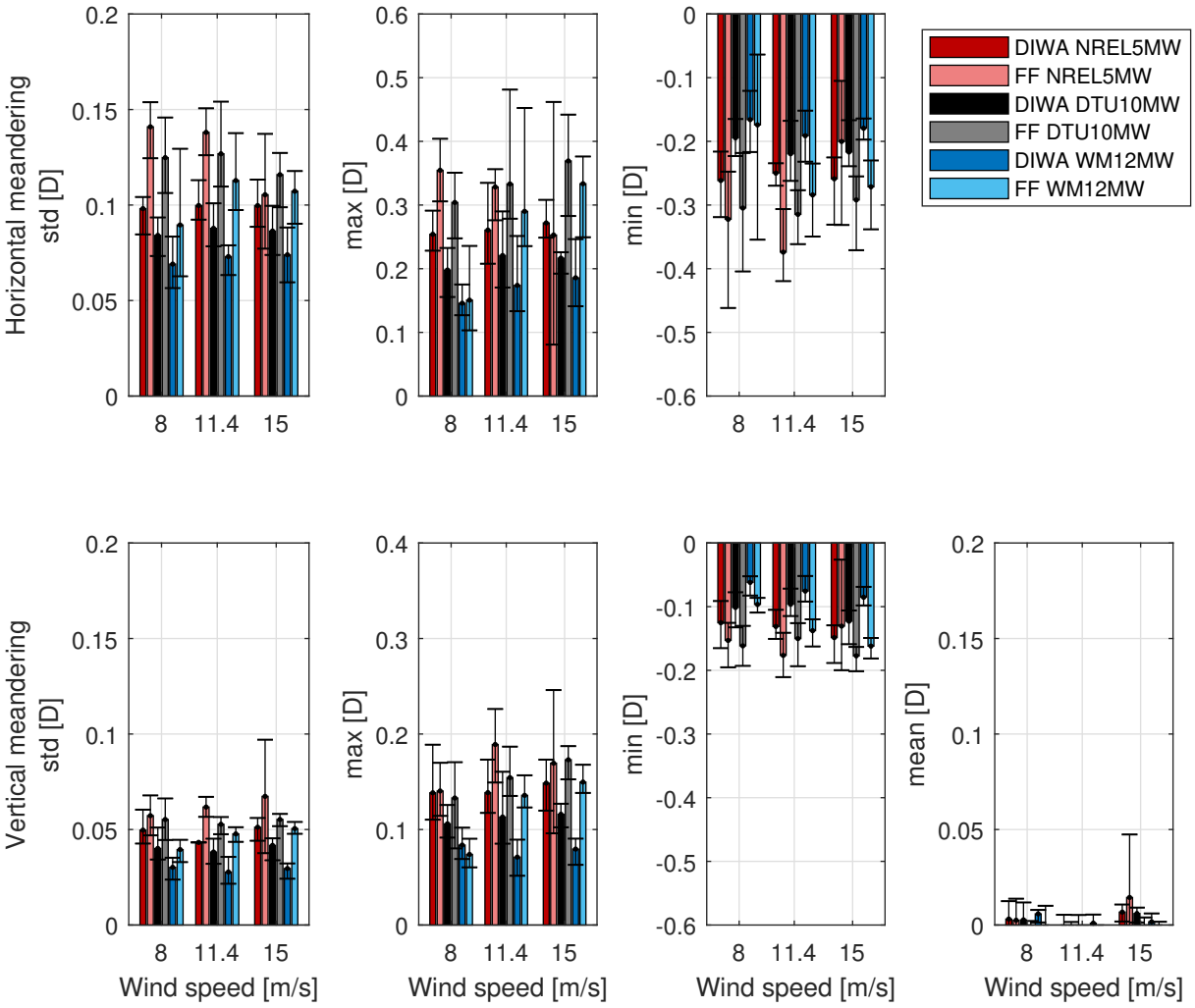

Figure 3: 1-hour meandering statistics for the three wind turbine models at 8D downstream. The hub height was subtracted to compute the vertical meandering statistical parameters.

sampled from the ambient wind field for one of the cases: the DTU10MW, for 11.4 m/s and one seed. The outcome is shown in Figure 6. The time series show the input wind fields used in both programs. The leftmost figure compares the ambient wind field at a node close to the hub to the meandering field in DIWA if it were down sampled (DS, in red), following the same approach as FAST.Farm does, and the meandering wind field without down sampling it (independently generated, in purple), i.e. following the recommended practice from the DWM model. The standard deviation is much lower in the latter case. However, the effect on the wake center PSD is not remarkable: as seen from the right subfigure in Figure 6, the difference between the programs in the frequency content is still there. The reported standard deviations of turbulence boxes are at the hub. However, the wind speeds that the wake center is subjected to are local and instantaneous, and therefore modifying the way the meandering turbulence box is generated does not have a significant effect, as seen from Figure 6.

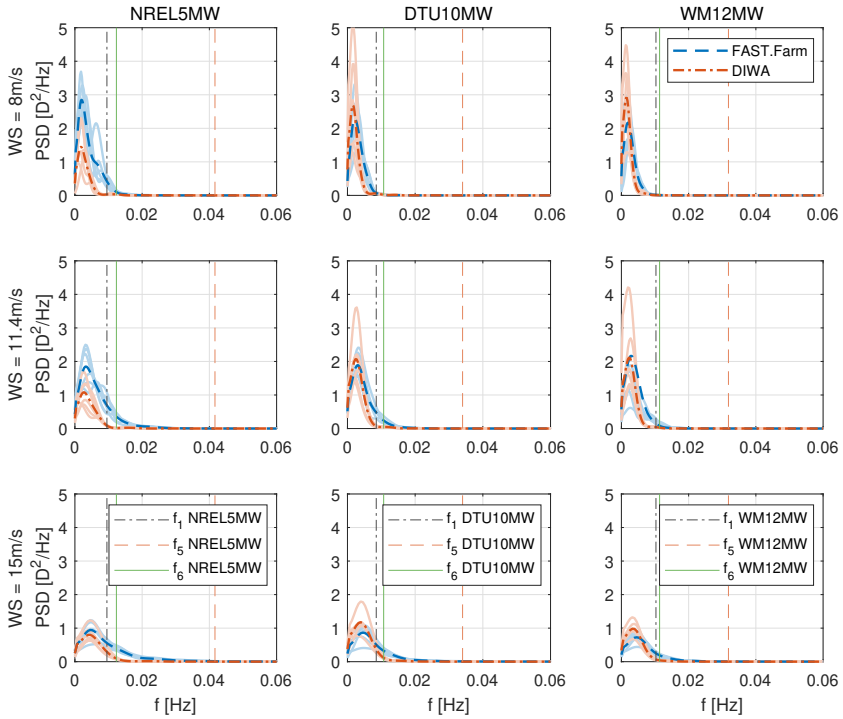

Figure 4: Power spectral density (PSD) of the horizontal wake center position at the target turbine for the three wind turbine models and the three wind speeds. The darker lines are the average of the six simulations for each case and the lighter lines are the results from individual realisations. The vertical lines represent the surge (f_1), pitch (f_5) and yaw (f_6) natural frequencies of three representative semisubmersible floaters for the respective rotor sizes.

3.3. Effect of tilt and precone in FAST.Farm

In comparisons against DIWA, the shaft tilt and the precone were set to zero when running FAST.Farm. However, if in FAST.Farm these values are not zero, the mean value of the vertical meandering is affected, especially for lower wind speeds. The statistics for the three wind turbine models, six realisations and the three wind speed conditions are presented in Figure 7, where the effect of tilt is shown. At 8 m/s, tilt causes the wake to move upward, as has already been reported in previous works [1]. This tendency is decreased as the wind speed increases.

3.4. Effect of including a shear profile in FAST.Farm

Similarly, FAST.Farm was run with a uniform shear profile when comparing against DIWA. When running FAST.Farm with a wind shear profile, a reduction in meandering for higher frequencies is observed. This effect is more pronounced as the wind speed increases, both for the vertical and horizontal meandering. Figure 8 shows this effect for the DTU10MW, one realisation and a mean wind speed of 11.4 m/s, with varying shear exponents α applied to a power-law profile.

This effect may be due to several factors: the wake planes move with the mean disturbed wind speed across the wake plane, and the turbulence box is advanced at the mean wind speed at the centre of the box (which is far above the hub-height [1]). Because of including shear, the mean wind speed across the wake plane will decrease or increase depending on the shear profile, while the wind speed at hub height is maintained the same for every case. Furthermore, since a higher shear yields a better wake recovery, the wake planes move at a different speed. This effect is higher the larger the wind speed is, as reported from Figure 8, and therefore the differences in the higher frequencies range are larger, which leads to a larger smoothening as the shear exponent increases.

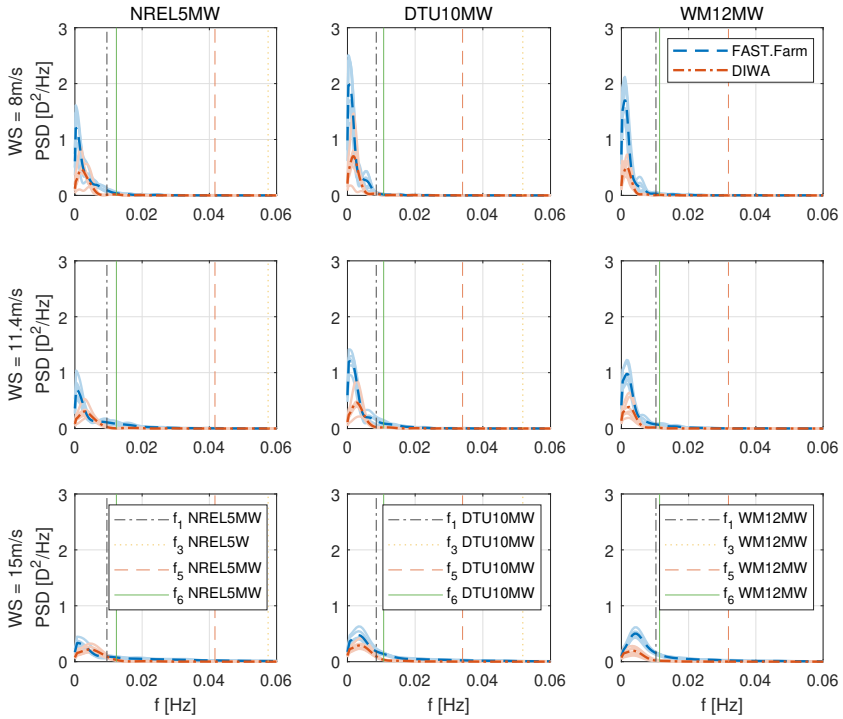

Figure 5: Power spectral density (PSD) of the vertical wake center position at the target turbine for the three wind turbine models and the three wind speeds. The darker lines are the average of the six simulations for each case and the lighter lines are the results from individual realisations. The vertical lines represent the surge (f_1), pitch (f_5), yaw (f_6) and heave (f_3) natural frequencies of three representative semisubmersible floaters for the respective rotor sizes.

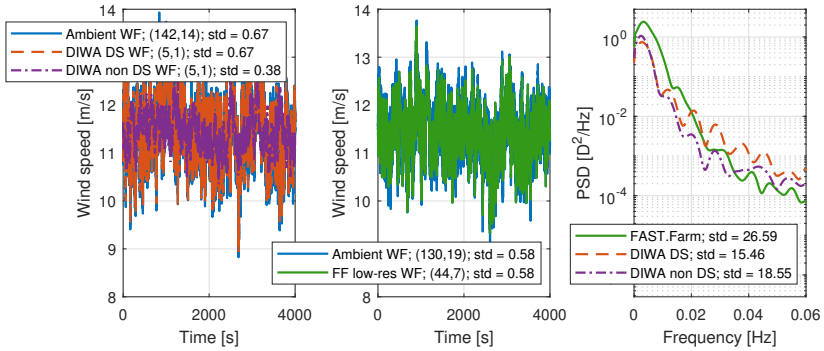

Figure 6: Left: time series of the ambient wind field at a node (in parentheses) close to the hub in DIWA, together with the meandering wind field if it is down sampled (DS WF) and in the case of being generated (non DS WF). Middle: ambient wind field at a node close to the hub in FAST.Farm, together with the low-resolution down sampled wind field. Right: wake center position PSD at 8D computed by FAST.Farm, DIWA if the meandering wind field is down sampled, and if it is generated.

4. Conclusions and further work

In the current work, we use the Dynamic Wake Meandering (DWM) model as implemented in two frameworks, DIWA and FAST.Farm, to study the low-frequency content of the meandering at a target turbine placed 8D downstream. Furthermore, the deficit at the target turbine as computed by FAST.Farm, and the four steady-state deficit models in DIWA, is presented. The wind speed across

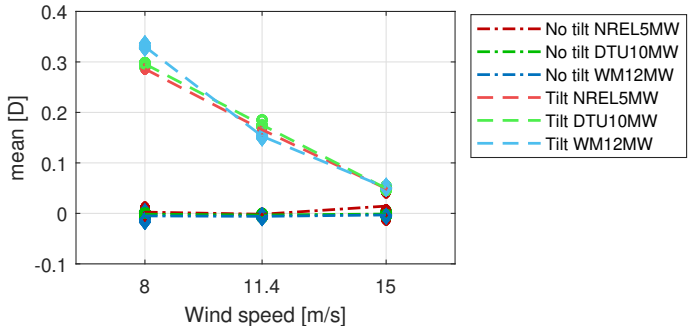

Figure 7: 1-hour mean of the vertical meandering for the case of having a tilt and precone and for the case of these values being zero, for the three wind speeds, for the three wind turbine models. The hub height was subtracted to compute the mean.

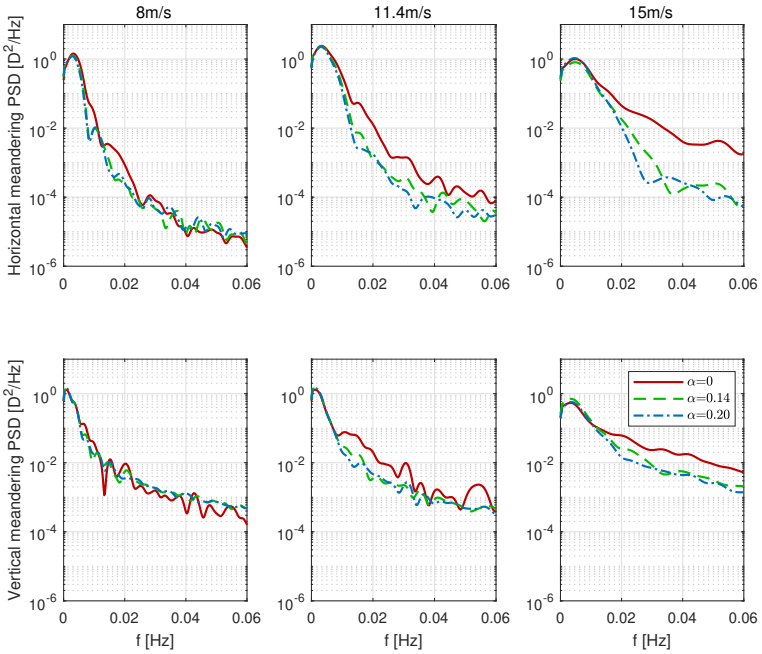

Figure 8: PSD of the vertical and horizontal wake center position for the case of having a shear profile with a power law exponent α of 0 (constant wind profile), 0.14 and 0.20. The results presented in this figure correspond to FAST.Farm simulations.

the rotor varies substantially depending on the wake deficit model applied, especially between the most recent model developed by Keck [10] and the one that was firstly implemented in the DWM model, i.e. the one from Madsen [9]. The faster wind speed recovery at the target turbine, if the former is applied, is consistent with previous findings in literature. Furthermore, it can account for atmospheric stability. The model included in the IEC standards [8] to calculate the deficit also accounts for atmospheric stability, as well as FAST.Farm, since it is based on specific user parameters that allow calibrating the model itself. Thus, at a later stage, these three models will be used to study what the effect of an unstable atmosphere is on the structural response of a semisubmersible, as already investigated for the Hywind spar FWT [25].

Concerning the meandering, the results show discrepancies at lower frequencies between the two frameworks. These differences are seen for every wind speed and wind turbine model, even though the differences decrease as the wind speed increases. To understand the effect of the difference in

frequency content at this range on a FWT in a wind farm is key, given the natural frequencies of the rigid body motions of floating wind substructures. From this work, we have not drawn any clear conclusion on where the differences may come from, but a fundamental difference is the way the wind field input is applied.

Another effect that has been observed in this work is the higher vertical meandering mean as the wind speed decreases if there is a rotor tilt angle. Furthermore, in FAST.Farm, if one applies a power-law shear profile to the ambient wind field, the frequency content at higher frequencies decreases, which yields a smoother horizontal and vertical meandering pattern. Further work is needed to identify the best way to consider the shear profile.

Acknowledgments
The research leading to these results has received funding from the Research Council of Norway through the ENERGIX programme (grant 294573) and industry partners Equinor, MacGregor, Inocean, APL Norway and RWE Renewables. Discussions with Jason Jonkman and Kelsey Shaler of NREL are also appreciated.

References

[1] Wise A S and Bachynski E E 2019 *Wind Energy*
[2] Ainslie J F 1988 *Journal of Wind Engineering and Industrial Aerodynamics* **27** 213–224
[3] España G, Aubrun S, Loyer S and Devinant P 2011 *Wind Energy* **14** 923–937
[4] Larsen G C, Madsen H A, Thomsen K and Larsen T J 2008 *Wind Energy* **11** 377–395
[5] Larsen T and Hansen A 2007 *How to HAWC2, the user's manual* Risø National Laboratory
[6] Larsen T J, Madsen H A, Larsen G C and Hansen K S 2012 *Wind Energy* **16** 605–624
[7] Larsen T J, Larsen G C, Helge A M and Petersen S M 2015 Wake effects above rated wind speed. An overlooked contributor to high loads in wind farms *Scientific Proceedings. EWEA Annual Conference and Exhibition 2015* (European Wind Energy Association (EWEA)) pp 95–99 ISBN 9782930670003 eWEA Annual Conference and Exhibition 2015 ; Conference date: 17-11-2015 Through 20-11-2015
[8] 2019 IEC61400-1: Wind energy generation systems– Part 1: Design requirements
[9] Madsen H A, Larsen G C, Larsen T J, Troldborg N and Mikkelsen R 2010 *Journal of Solar Energy Engineering* **132**
[10] Keck R E 2013 *A consistent turbulence formulation for the dynamic wake meandering model in the atmospheric boundary layer* Ph.D. thesis DTU Denmark
[11] Jonkman J M, Annoni J, Hayman G, Jonkman B and Purkayastha A 2017 Development of FAST.Farm: a new multi-physics engineering tool for wind-farm design and analysis *35th Wind Energy Symposium* (American Institute of Aeronautics and Astronautics)
[12] SINTEF Ocean 2020 *DIWA-Park Dynamic Wake Meandering (DWM) Theory Manual*
[13] Jonkman J, Butterfield S, Musial W and Scott G 2009 Definition of a 5-MW reference wind turbine for offshore system development Tech. rep. NREL
[14] Bak C, Zahle F, Bitsche R, Kim T, Yde A, Henriksen L C, Natarajan A and Hansen M H 2013 The DTU 10MW reference wind turbine project site accessed 01.08.2019. URL `http://dtu-10mw-rwt.vindenergi.dtu.dk`
[15] de Souza C and Berthelsen P 2020 SIMA model of the Windmoor 12 MW base case FWT v1.1. Tech. rep. SINTEF Ocean
[16] Jiménez A, Crespo A and Migoya E 2009 *Wind Energy* **13** 559–572
[17] Jonkman J, Doubrawa P, Hamilton N, Annoni J and Fleming P 2018 *Journal of Physics: Conference Series* **1037** 062005
[18] Doubrawa P, Annoni J R and Jonkman J M 2018 Optimization-based calibration of FAST.Farm parameters against Large-Eddy Simulations *2018 Wind Energy Symposium* (American Institute of Aeronautics and Astronautics)
[19] Shaler K, Jonkman J and Hamilton N 2019 *Journal of Physics: Conference Series* **1256** 012023
[20] Panjwani B, Kvittem M, Eliassen L, Ormberg H and Godvik M 2019 *Journal of Physics: Conference Series* **1356** 012039
[21] Monin A S and Obukhov A M 1954 *Contrib. Geophys. Inst. Acad. Sci. USSR* **24** 163–187
[22] 2020 Bundesamt für Seeschifffahrt und Hydrographie FINO - Databankinformationen
[23] Robertson A N, Wendt F, Jonkman J M, Popko W, Dagher H, Gueydon S, Qvist J, Vittori F, Azcona J, Uzunoglu E, Soares C G, Harries R, Yde A, Galinos C, Hermans K, de Vaal J B, Bozonnet P, Bouy L, Bayati I, Bergua R, Galvan J, Mendikoa I, Sanchez C B, Shin H, Oh S, Molins C and Debruyne Y 2017 *Energy Procedia* **137** 38 – 57 ISSN 1876-6102 14th Deep Sea Offshore Wind R&D Conference, EERA DeepWind'2017
[24] Pegalajar-Jurado A, Madsen F, Borg M and Bredmose H 2018 Public definition of the two LIFE 50+ 10MW floater concepts Tech. rep. Lifes50+
[25] Jacobsen A and Godvik M 2020 *Wind Energy*

Appendix

Table 5: Recommended and applied values for the spatial and time resolution in the wind field generation.

	8 m/s				**11.4 m/s**				**15 m/s**			
	NREL5MW											
	FAST.Farm		DIWA		FAST.Farm		DIWA		FAST.Farm		DIWA	
	Rec.	Used	Rec.	Used	Rec.	Used	Rec.	Used	Rec.	Used	Rec.	Used
dxLow [m]	0.079D	0.238D	2-8	8	0.16D	0.23D	2.85-11.4	11.4	0.24D	0.18D	3.75-15	15
dSLow [m]	0.079D	0.079D	1D	1.07D	0.16D	0.12D	1D	1.07D	0.24D	0.20D	1D	1.07D
dxHigh [m]	-	3.75	-	3.75	-	2.85	-	2.85	-	1.50	-	1.50
dSHigh [m]	5	5	5	5	5	5	5	5	5	5	5	5
DtLow [s]	0.024D	0.030D	-*	1 s	0.016D	0.023D	-*	1 s	0.0079D	0.012D	-*	1 s
DtHigh [s]	-	0.25	-	0.25	-	0.25	-	0.25	-	0.25	-	0.25
	DTU10MW											
	FAST.Farm		DIWA		FAST.Farm		DIWA		FAST.Farm		DIWA	
	Rec.	Used	Rec.	Used	Rec.	Used	Rec.	Used	Rec.	Used	Rec.	Used
dxLow [m]	0.079D	0.168D	2-8	8	0.16D	0.16D	2.85-11.4	11.4	0.24D	0.13D	3.75-15	15
dSLow [m]	0.079D	0.084D	1D	1.14D	0.16D	0.13D	1D	1.14D	0.24D	0.21D	1D	1.14D
dxHigh [m]	-	3.75	-	3.75	-	2.85	-	2.85	-	1.50	-	1.50
dSHigh [m]	5	7.5	5	7.5	5	7.5	5	7.5	5	7.5	5	7.5
DtLow	0.024D	0.021D	-*	1 s	0.016D	0.014D	-*	1 s	0.0079D	0.008D	-*	1 s
DtHigh [s]	-	0.25	-	0.25	-	0.25	-	0.25	-	0.25	-	0.25
	WM12MW											
	FAST.Farm		DIWA		FAST.Farm		DIWA		FAST.Farm		DIWA	
	Rec.	Used	Rec.	Used	Rec.	Used	Rec.	Used	Rec.	Used	Rec.	Used
dxLow [m]	0.079D	0.138D	2-8	8	0.16D	0.13D	2.85-11.4	11.4	0.24D	0.104D	3.75-15	15
dSLow [m]	0.079D	0.069D	1D	0.94D	0.16D	0.11D	1D	0.94D	0.24D	0.17D	1D	0.94D
dxHigh [m]	-	3.75	-	3.75	-	2.85	-	2.85	-	1.50	-	1.50
dSHigh [m]	5	7.5	5	7.5	5	7.5	5	7.5	5	7.5	5	7.5
DtLow	0.024D	0.017D	-*	1 s	0.016D	0.011D	-*	1s	0.0079D	0.0069D	-*	1 s
DtHigh [s]	-	0.25	-	0.25	-	0.25	-	0.25	-	0.25	-	0.25

* Based on dxLow.